Revue Roumaine de Chimie, **2008**, *53*(12), 1149–1156

THE "PUSH" EFFECT OF THE THIOLATE AXIAL LIGAND IN SUPEROXIDE REDUCTASE: A DENSITY FUNCTIONAL STUDY

Radu SILAGHI-DUMITRESCU

"Babeş-Bolyai" University, Faculty of Chemistry and Chemical Engineering,
11 Arany Janos street, Cluj-Napoca RO-400028, Roumania

Received May 15, 2008

Superoxide reductases and cytochromes P450 share a common motif at their active sites: a ferrous center with FeN_4S coordination, where the thiolate occupies an axial position, trans to the substrate binding site. A thiolate "push effect" has been proposed responsible for the apparently orthogonal reactivities of P450 and SOR ferric-hydroperoxo catalytic intermediates: promoting O-O bond cleavage (in P450), and promoting Fe-O bond cleavage (in SOR). Reported here are DFT geometry optimization results on ferric-(hydro)peroxo models of the SOR active site, with the axial thiolate replaced by various neutral or anionic ligands, suggesting only a moderate thiolate trans effect on the iron-(hydro)peroxo bonding. On the other hand, the same computational methodology demonstrates a dramatic trans effect of the thiolate in SOR ferrous-nitric oxide adducts (via a strong S-Fe π interaction), in agreement with a recent experimental report showing evidence for a sizeable thiolate push-effect in the nitric oxide adduct of the SOR site. The proton affinity of the ferric-peroxo models is some 200 kca/mol higher in the mode featuring a thiolate axial ligand, compared to the modes featuring a neutral amine ligand. This thermodynamic factor may well become the key reason why an enzyme like SOR would prefer an axial cysteinate ligand: such a ligand would distinctly accelerate peroxide protonation, thus allowing for a more efficient turnover.

INTRODUCTION

Superoxide reductases[1,2] and cytochromes P450[3] share a common motif at their active sites: a ferrous center with FeN_4S coordination, where a thiolate sulfur occupies an axial position, trans to the substrate binding site (Fig. 1). The four nitrogen atoms belong to a porphyrin in P450 and to four equatorial histidine side-chains in SOR.

Fig. 1 illustrates the proposed catalytic cycles of SOR[4,5] and P450[3]. Two apparently orthogonal functions have been proposed for the thiolate ligand in P450 and SOR ferric-peroxo catalytic intermediates, under a framework known as "the push effect".[6] Thus, at the ferric-hydroperoxo level, the thiolate is assumed to facilitate O-O bond cleavage in P450[3,7] as opposed to Fe-O bond cleavage in SOR.[8,9]

It was previously reported[5] that the trans ("push") effect of the thiolate in heme-(hydro)peroxo adducts appears to be small at the geometric level. Thus, thiolate-ligated "ferric-peroxo" and ferric-hydroperoxo complexes featured Fe-O and O-O bond lengths very similar to those where the thiolate was replaced by imidazole, imidazolate, or phenoxide.[5] Slightly longer Fe-O *and* O-O bonds were noted in thiolate compared to non-thiolate models, possibly indicating an electronic basis for the proposed[8,9] apparently orthogonal facets of the "push effect": Fe-O bond cleavage and O-O bond cleavage. On the other hand, the energetics of the "ferrous-dioxygen" – "ferric-peroxo" – ferric-hydroperoxo sequence were clearly different with thiolate compared to imidazole.[5] As expected based on simple charge arguments, the thiolate-ligated "ferric-peroxo" adduct had a much higher proton affinity than its imidazole-ligated counterpart. Along the same lines, reduction of "ferrous-dioxygen" to "ferric-peroxo" was harder to accomplish in thiolate models than in imidazole models.[5] The latter feature, which we described as "thiolate obstruction", appears to also be active in nitric oxide reduction by another heme-thiolate active enzyme, P450nor, and its physiological utility as a "control switch" has been pointed out.[10] For other facets of the "thiolate push", the reader is referred to extensive investigations by Shaik and co-workers.[7]

* Corresponding author: fax: +40-264-590818, e-mail: rsilaghi@chem.ubbcluj.ro

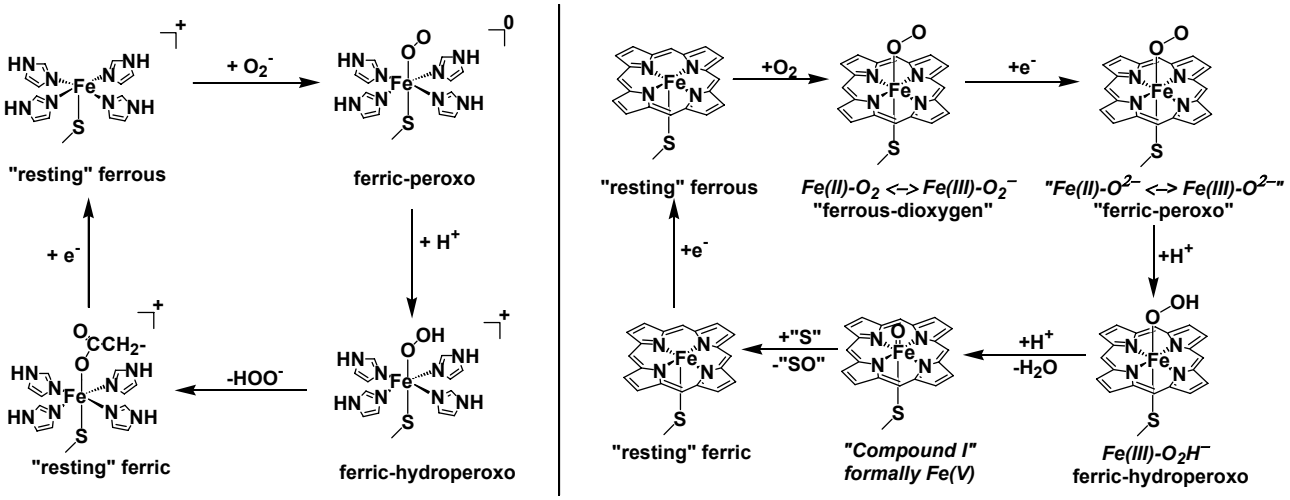

Fig. 1 – Proposed catalytic cycles of SOR (left) and P450 (right). For P450, "S" is a generic organic substrate that undergoes oxygen atom insertion to yield "SO".

Upon describing the ferric-peroxo and ferric-hydroperoxo adducts of SOR, it was previously pointed out that their Fe-O bonds appeared in no way different from those of other ferric-peroxo models. We therefore proposed a key role for *solvent* in promoting indiscriminate protonation of these SOR-peroxo intermediates, thereby favoring product (*i.e.*, peroxide) liberation.[11] This solvent exposure was contrasted to the controlled proton delivery machinery in the buried P450 active site,[3,12] where selective protonation of the terminal oxygen atom in the ferric-hydroperoxo intermediate leads to O-O bond cleavage. This explanation proposal was further supported by Kovacs and co-workers,[9] who in addition reported an SOR ferric-hydroperoxo model compound that was low-spin, and which underwent rapid Fe-O bond cleavage but no detectable O-O bond cleavage.[13] These findings have thus suggested a negligible role for the thiolate in SOR, as opposed to P450. Others[8,9] have however proposed a key the role of the thiolate in SOR, as favoring the high-spin versus the low-spin state for the ferric-hydroperoxo catalytic intermediate. Indeed, as confirmed by density functional calculations,[11] high-spin SOR ferric (hydro)peroxo models feature significantly weaker Fe-O bonds than their low-spin counterparts. Here, we demonstrate that the two apparently conflicting interpretations of the importance of the thiolate ligand, one drawn from computational data on SOR peroxo models and one drawn from spectroscopic examination of inhibitor-bound SOR sites, in fact offer two facets of the same coin. DFT geometry optimization data are reported on ferric-(hydro)peroxo models of the SOR active site, where the axial thiolate has been replaced by neutral or anionic ligands. We find that these replacements yield no evidence for a significant thiolate trans effect on the peroxo (hydro)ligand. We then report DFT data on the nitric oxide adduct of the SOR site, and attempt to correlate these parameters with the peroxo models. We report a dramatic trans effect of the thiolate in the SOR-NO adduct. Examining SOR-NO models with different axial ligands, we assign the trans effect to a strong S-Fe π interaction. The data reported here allows a detailed "unified" electronic interpretation of the thiolate push.

MATERIALS AND METHODS

The UBP86 functional (the gradient-corrected exchange functional of Becke (1988),[14] the correlation functional of Perdew (1986)[15]), and the DN** numerical basis set (comparable in size to 6-31G**) were used.[16] In SCF calculations, a fine grid was used; the convergence criteria were 10^{-6} (root-mean square of electron density) and 10^{-8} (energy), respectively. For geometry optimization, convergence criteria were 0.001 au (maximum gradient criterion) and 0.0003 (maximum displacement criterion).

All models (shown in Fig. 2) were subjected to full geometry optimization, without any geometry or symmetry constraints. When previously reporting DFT data on SOR models, we used protonated imidazoles to model the histidine ligands present at the active site, and we pointed out that orientation of the imidazole planes was important in obtaining a meaningful picture of the SOR mechanism.[11] In the same study, the

orientation of the methyl-sulfur bond relative to the iron-nitrogen bonds was also found to be important. Here, we examine models where the axial methyl-thiolate ligand is replaced by ammonia, methoxy, or thiophenol moieties. Since the steric demands of these ligands vary, we choose not to employ any geometry constraints in optimizing geometries for the models reported here. This then also allows us to use ammonia as the equatorial ligands instead of the imidazoles used in our previous study. Results on selected key models in fact showed that this replacement had little effect on the conclusions of the study,[17] and therefore we do not discuss the equatorial imidazole models any further.

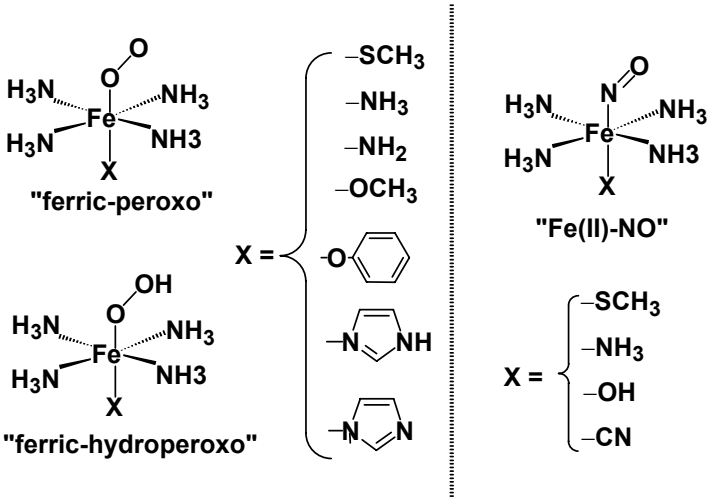

Fig. 2 – Models employed in the present study.

RESULTS

Table 1 shows the computed geometrical parameters for ferric-peroxo (hereafter refered to as $[FeO_2]^8$]) and ferric-hydroperoxo (hereafter referred to as $[FeO_2H]^8$]) models with various ligands (cf. Figure 2).

The Fe-O and O-O distances shown in Table 1 correlate well with our previous findings[5] on the related $[FeO_2]^8$ and $[FeO_2H]^8$ heme models with similar axial ligands. Thus, the thiolate appears more efficient than imidazole, phenoxide, ammonia, or imidazolate, in "pushing electrons" into the Fe-O-O(H) antibonding orbitals, a push that increases[5] the Fe-O and O-OH bond lengths. On the other hand, the O-O bonds in the amido and methoxy models appear to testify for an even more efficient push than in the thiolate models. We note that the O-O bonds for $[FeO_2]^8$ models generally appear longer than in the larger models previously reported[11] by us. This is due to the proximity of the (equatorial) ammonia protons to the peroxo ligand, which allows for two NH-O hydrogen bonds in the models $[FeO_2]^8$ of Fig. 2; by contrast, previously reported models featuring imidazole equatorial ligands[11] only offered CH protons for hydrogen bonding to the peroxo ligand. Since the SOR active site is solvent-exposed[18,19] and therefore available for hydrogen bonding, the small models examined here are likely to yield a more realistic account of the O-O bond length than the larger models previously reported.[11] As such, the data shown here further argues towards a peroxo, and not superoxo,[11] description of the ligand in the putative $[FeO_2]^8$ complexes.

A recently emerged paradigm states that low-spin ferric-hydroperoxo complexes are ideally suited for O-O bond cleavage, whereas high-spin ferric-hydroperoxo complexes are ideally suited for Fe-O bond cleavage.[20,21] It has therefore been proposed[8,9] that an SOR ferric-hydroperoxo adduct must be high-spin, since the physiological function of SOR involves not O-O bond cleavage, but rather Fe-O bond cleavage. A key role for the thiolate axial ligand has been proposed in favoring this high-spin state.[8,9] Indeed, our data (Table 1) illustrates how high-spin $[FeO_2H]^8$ adducts feature a particularly weaker bond than their low-spin counterparts, while also featuring a shorter (and presumably stronger) O-O bond. Furthermore, the low-spin/high-spin balance seems to be more efficiently pushed towards high-spin by a thiolate than by imidazole (Table 1). However, other biologically-relevant ligands (methoxide and phenoxide, mimicking serine, threonine and tyrosine) would be even more efficient in this

respect. Furthermore, for all models reported here, as well as for larger SOR models previously described,[11] low-spin $[FeO_2H]^8$ appears to be clearly energetically favored over high-spin. This latter observation may in principle be assigned to a systematic error in our calculated relative energies;[9] under such an assumption, the *rest* of our data would then support the "high-spin theory". In fact, in line with the classical push theory[3,6] as well as in line with the "thiolate high-spin theory",[8,9] our unpublished calculations indeed suggest a relatively low energy barrier for O-O bond cleavage in S=1/2 thiolate-Fe(III)-OOH, slightly lower than in both S=5/2 thiolate-Fe(III)-OOH and S=1/2 ammonia(non-thiolate)-Fe(III)-OOH. However solvent exposure of the SOR site may in fact result in a rapid proton-driven liberation of peroxide, that would out-compete an otherwise possible O-O bond cleavage.[11]

Table 1

Energies (kcal/mol) and key distances (Å)
for ferric-(hydro)peroxo models shown in Fig. 2

Model	Axial ligand	Energy	Fe-O	O-O	Fe-X
S=1/2 $[FeO_2]^8$	-SCH_3	-1304637.5	1.86	1.42	2.33
S=5/2 $[FeO_2]^8$	-SCH_3	-1304622.0	1.99	1.40	2.34
S=1/2 $[FeO_2H]^8$	-SCH_3	-1304907.9	1.84	1.52	2.24
S=5/2 $[FeO_2H]^8$	-SCH_3	-1304891.0	1.96	1.46	2.33
S=1/2 $[FeO_2]^8$	-OCH_3	-1101936.0	1.84	1.43	1.97
S=5/2 $[FeO_2]^8$	-OCH_3	-1101924.1	1.97	1.43	1.93
S=1/2 $[FeO_2H]^8$	-OCH_3	-1102209.1	1.81	1.53	1.87
S=5/2 $[FeO_2H]^8$	-OCH_3	-1102197.8	1.94	1.46	1.86
S=1/2 $[FeO_2]^8$	-NH_3	-1065059.0	1.83	1.38	2.14
S=5/2 $[FeO_2]^8$	-NH_3	-1065043.8	1.92	1.34	2.29
S=1/2 $[FeO_2H]^8$	-NH_3	-1065234.6	1.79	1.47	2.10
S=5/2 $[FeO_2H]^8$	-NH_3	-1065218.5	1.92	1.42	2.26
S=1/2 $[FeO_2]^8$	-NH_2	-1064781.3	1.85	1.44	1.99
S=5/2 $[FeO_2]^8$	-NH_2	-1064768.7	1.94	1.42	1.95
S=1/2 $[FeO_2H]^8$	-NH_2	-1065059.3	1.83	1.54	1.88
S=5/2 $[FeO_2H]^8$	-NH_2	-1065045.2	1.96	1.47	1.93
S=1/2 $[FeO_2]^8$	-Im	-1171305.8	1.84	1.41	2.02
S=5/2 $[FeO_2]^8$	-Im	-1171280.7	1.85	1.34	2.09
S=1/2 $[FeO_2H]^8$	-Im	-1171567.3	1.81	1.52	1.94
S=5/2 $[FeO_2H]^8$	-Im	-1171546.5	1.94	1.46	2.06
S=1/2 $[FeO_2]^8$	-ImH	-1171572.5	1.83	1.38	2.07
S=5/2 $[FeO_2]^8$	-ImH	-1171554.9	1.91	1.35	2.21
S=1/2 $[FeO_2H]^8$	-ImH	-1171758.5	1.79	1.48	2.04
S=5/2 $[FeO_2H]^8$	-ImH	-1171739.0	1.92	1.42	2.18
S=1/2 $[FeO_2]^8$	-OPh	-1222307.3	1.82	1.42	2.01
S=5/2 $[FeO_2]^8$	-OPh	-1222290.2	1.85	1.35	2.05
S=1/2 $[FeO_2H]^8$	-OPh	-1222579.2	1.80	1.53	1.91
S=5/2 $[FeO_2H]^8$	-OPh	-1222569.0	1.94	1.47	1.89

The partial atomic charges and spin densities on the peroxo ligand offer another measure of the axial ligand "push". Table 2 illustrates these values for the models of Fig. 2. The general trend is evident, that anionic ligands induce more charge and less spin accumulation on the peroxo ligand, consistent with favoring a peroxo character vs. superoxo. In this respect, amide and thiolate appear to be most efficient. By contrast, neutral ligands (NH_3 and imidazole) feature significantly higher spin density and significantly less charge on the OOH ligand in the $[FeO_2H]^8$ models. Thus, anionic ligands appear particularly suited for the SOR catalytic cycle, where commitment towards formation of peroxide is desirable upon substrate (superoxide) binding to the ferrous active site (cf. Fig. 1). These trends in partial atomic charges were also noted for the equivalent heme models (with axial thiolate, phenoxide, imidazole, or imidazolate ligands).[5] The larger set of models available now allows us to more closely examine the electronic details of the "thiolate push effect". Thiolate being a very covalent ligand, is likely to mix its orbitals with the iron, creating lower-energy doubly-occupied orbitals that have considerable iron character, as well as higher-energy singly-occupied (or empty, depending on spin and oxidation state) orbitals that were originally 100% iron, but have now acquired significant sulfur character form covalent mixing. The participation of iron in the

low-energy doubly-occupied bonding orbitals must result in an increase in total electron density on the iron, compared to a "reference" state where no iron-sulfur mixing would occur. This increased electron density has been probed experimentally, and is consistently illustrated by data in Table 2 and by previously reported data on similar heme models.[22] However, this increased electron density on iron is unlikely to have a great effect on reactivity towards incoming exogenous ligands, since the bonding orbitals discussed here would be low in energy. Instead, the iron-sulfur antibonding orbitals will be higher in energy and therefore involved in binding a sixth ligand trans to the sulfur. We can see that the same covalence that leads to electron enrichment of the iron via the bonding orbitals, leaves the antibonding orbitals with less iron character. In other words, the thiolate (covalent ligands in general) in fact decreases the ability of the iron to efficiently interact with incoming ligands. This then explains why the iron-peroxo distances are longer with a thiolate than with any other axial ligand (cf. Table 1 and Refs). This trend contrasts that seen with partial atomic charges on the peroxo moiety. Compared to the thiolate, the less covalent (harder) anionic ligands such methoxide and amide in fact induce charges either as high, or higher, on the peroxide. We must conclude that the apparent "electron push" seen with these anionic ligands must have a significant charge component, and may have little to do with covalence. There are, therefore, three independent factors at work here. First, the thiolate-iron bonding orbitals, which increase electron density at the iron; these bonding orbitals thus justify the "thiolate push" notion, but this must have little relevance for reactivity. Second, the thiolate-iron antibonding orbitals feature decreased iron character; thus effectively pulling away electron density from the high-lying iron orbital, reducing its efficiency in interacting with incoming ligands; thus, reactivity-wise, "thiolate pull" would be a more appropriate term than "thiolate push". Third, there is a purely electrostatic component, having to do with the negative charge of the thiolate. Unlike the previous two components of the "thiolate push", the electrostatic component is present with any anionic ligand. Its efficiency, however, decreases with increasing size of the axial ligand. Implicitly, thiolate would have a stronger electrostatic component than phenoxide. This electrostatic component in fact becomes a key factor in catalytic cycles of enzymes where one electron reduction of "ferrous-dioxygen" to "ferric-peroxo" is required. In these cases, a "thiolate obstruction" effect is seen, where the strong electrostatic component described above, hampers electron transfer. The three components enumerated above also explain differences between thiolate and imidazole complexes. As a general conclusion on the "thiolate push" we can see that the two components of this effect that are the most relevant to ligand binding, act to diminish reactivity ("thiolate pull", "thiolate obstruction").

Other facets of the "push effect" were described in great detail elsewhere.[7] It is, for instance, known that thiolate-ligated Compound I (resulted from heterolytic cleavage of the O-OH bond in ferric-hydroperoxo complexes, cf. Fig. 1) is more adept than histidine-ligated Compound I at transferring its oxygen atom towards organic substrates.[3] While the reaction pathways for these two Compound I species were described in great detail,[7] we will simply mention the "greater picture": thiolate-ligated Compound I is S=1/2 (a Fe(IV)-oxo moiety antiferromagnetically coupled to a porphyrin cation radical), whereas imidazole-ligated Compound I is S=3/2 (with ferromagnetic coupling between Fe(IV)-oxo and the porphyrin cation radical).[23] The origin of this difference was shown to again lie in the strongly covalent Fe-S interaction.[23] It is precisely this difference in spin states that readily explains the different reactivities of thiolate vs. imidazole Compound I, in the mono-oxygenase reaction shown in Fig. 1. S=1/2 thiolate Compound I reacting with an organic substrate would produce a substrate-bound S=1/2 Fe(III), which conserves spin. S=3/2 imidazole Compound I would instead produce product and S=3/2 Fe(III), which is essentially an excited state and would further need to cross over to different spin surfaces, thus breaking the "spin conservation" rule.

The computational data available thus far on the SOR-(hydro)peroxo adducts appears to reveal only a moderate role for the thiolate in "pushing electrons" onto the peroxide or in favoring high-spin states. However, experimental data on an SOR ferrous-nitrosyl ($[FeNO]^7$) adduct[8] has revealed evidence for a thiolate trans effect, manifested in weakening of the Fe-NO and N-O bonds compared to other $[FeNO]^7$ complexes, as well as in an intrinsic instability of the SOR $[FeNO]^7$ adduct. To reconcile theory with experiment, we have examined the $[FeNO]^7$ SOR-NO adduct with the same computational methodology employed for the peroxo models. Table 3 shows computed geometries for SOR-NO models assuming axial thiolate, NH_3, cyanide, or hydroxide ligands.[24] A striking feature of the thiolate model is its

extremely long (2.04 Å) Fe-NO bond, which is ~0.3 longer than normally seen in Fe(II)-NO adducts.[10,25-29] By contrast, all other ligands examined here yield a canonical Fe-NO distance at 1.77-1.78 Å. Taken together, the cyanide, ammonia, and hydroxide models offer trans axial ligands of widely varying strength, charge, and bonding type. None of these ligands appear to mimic even closely the unusually long Fe-NO bond of the thiolate model. It has previously been argued that the intrinsic softness of the thiolate ligand would impose a high-spin state on the iron, thereby favoring a high-spin hydroperoxo intermediate in the SOR catalytic cycle.[8,9] However, the identical bond lengths between the hydroxo and the cyano SOR-NO models suggest that ligand softness cannot be made responsible for any significant elongation of the Fe-NO bond in SOR-NO. What makes the thiolate so unique? An unexpectedly clear-cut answer comes from comparative examination of the frontier molecular orbitals in SOR-NO models with various axial ligands, where strong iron-sulfur covalence is seen to effectively prevent efficient Fe-NO bonding. By contrast, the non-thiolate SOR-NO models feature extremely covalent Fe-N-O units, with σ and π bonding consistent with previous reports on other [FeNO]^7 systems.

Table 2

Partial atomic charges and spin densities on the iron and peroxide for models shown in Fig. 2. Spin densities are shown in parentheses

Model	Axial ligand	Fe	O1[a]	O2[b]	OO(H)[c]
S=1/2 $[FeO_2]^8$	$-SCH_3$	0.43 (0.56)	-0.32 (0.19)	-0.46 (0.26)	-0.79 (0.45)
S=5/2 $[FeO_2]^8$	$-SCH_3$	0.75 (3.80)	-0.37 (0.31)	-0.43 (0.44)	-0.80 (0.75)
S=1/2 $[FeO_2H]^8$	$-SCH_3$	0.44 (0.71)	-0.39 (0.15)	-0.34 (0.02)	-0.42 (0.17)
S=5/2 $[FeO_2H]^8$	$-SCH_3$	0.79 (3.89)	-0.41 (0.33)	-0.27 (0.08)	-0.38 (0.41)
S=1/2 $[FeO_2]^8$	$-OCH_3$	0.55 (0.57)	-0.33 (0.26)	-0.46 (0.19)	-0.79 (0.45)
S=5/2 $[FeO_2]^8$	$-OCH_3$	0.88 (3.84)	-0.38 (0.32)	-0.44 (0.41)	-0.82 (0.74)
S=1/2 $[FeO_2H]^8$	$-OCH_3$	0.61 (0.74)	-0.38 (0.16)	-0.33 (0.02)	-0.41 (0.18)
S=5/2 $[FeO_2H]^8$	$-OCH_3$	0.97 (3.97)	-0.43 (0.31)	-0.27 (0.07)	-0.40 (0.38)
S=1/2 $[FeO_2]^8$	$-NH_3$	0.52 (0.44)	-0.26 (0.29)	-0.37 (0.29)	-0.67 (0.58)
S=5/2 $[FeO_2]^8$	$-NH_3$	0.75 (3.68)	-0.27 (0.56)	-0.27 (0.55)	-0.54 (1.01)
S=1/2 $[FeO_2H]^8$	$-NH_3$	0.59 (0.71)	-0.29 (0.27)	-0.26 (0.09)	-0.21 (0.36)
S=5/2 $[FeO_2H]^8$	$-NH_3$	0.96 (4.03)	-0.32 (0.46)	-0.21 (0.16)	-0.18 (0.62)
S=1/2 $[FeO_2]^8$	$-NH_2$	0.52 (0.62)	-0.34 (0.24)	-0.48 (0.15)	-0.82 (0.39)
S=5/2 $[FeO_2]^8$	$-NH_2$	0.84 (3.87)	-0.39 (0.40)	-0.46 (0.26)	-0.85 (0.66)
S=1/2 $[FeO_2H]^8$	$-NH_2$	0.57 (0.68)	-0.41 (0.11)	-0.36 (0.01)	-0.47 (0.12)
S=5/2 $[FeO_2H]^8$	$-NH_2$	0.91 (3.96)	-0.42 (0.29)	-0.30 (0.06)	-0.41 (0.35)
S=1/2 $[FeO_2]^8$	-Im	0.53 (0.52)	-0.30 (0.28)	-0.44 (0.22)	-0.74 (0.50)
S=5/2 $[FeO_2]^8$	-Im	0.81 (3.70)	-0.30 (0.53)	-0.35 (0.56)	-0.65 (1.15)
S=1/2 $[FeO_2H]^8$	-Im	0.60 (0.73)	-0.36 (0.19)	-0.34 (0.03)	-0.40 (0.22)
S=5/2 $[FeO_2H]^8$	-Im	0.73 (3.77)	-0.41 (0.31)	-0.29 (0.07)	-0.59 (0.38)
S=1/2 $[FeO_2]^8$	-ImH	0.52 (0.41)	-0.26 (0.30)	-0.37 (0.29)	-0.63 (0.59)
S=5/2 $[FeO_2]^8$	-ImH	0.83 (3.75)	-0.29 (0.54)	-0.33 (0.49)	-0.62 (1.03)
S=1/2 $[FeO_2H]^8$	-ImH	0.60 (0.72)	-0.29 (0.26)	-0.28 (0.08)	-0.27 (0.34)
S=5/2 $[FeO_2H]^8$	-ImH	0.97 (4.05)	-0.33 (0.43)	-0.22 (0.13)	-0.21 (0.58)
S=1/2 $[FeO_2]^8$	-OPh	0.55 (0.52)	-0.30 (0.22)	-0.45 (0.28)	-0.75 (0.50)
S=5/2 $[FeO_2]^8$	-OPh	0.81 (3.68)	-0.30 (0.53)	-0.36 (0.55)	-0.66 (1.08)
S=1/2 $[FeO_2H]^8$	-OPh	0.61 (0.71)	-0.37 (0.18)	-0.33 (0.03)	-0.40 (0.21)
S=5/2 $[FeO_2H]^8$	-OPh	0.96 (3.94)	-0.43 (0.30)	-0.28 (0.06)	-0.41 (0.36)

[a]iron-bound oxygen. [b]non iron-bound oxygen. [c]sum over the OO(H) ligand.

Table 3

Computed geometrical parameters for SOR-NO models with various axial ligands (cf. Fig. 2). Distances are given in Å, angles in degrees

X[a]	Fe-NO	Fe-N-O	N-O	Fe-X
SCH_3^-	2.04[30]	125	1.23	2.22
OH^-	1.76	142	1.19	1.95
NH_3	1.77	151	1.17	2.25
CN^-	1.77	143	1.18	2.02

[a] axial ligand trans to NO.

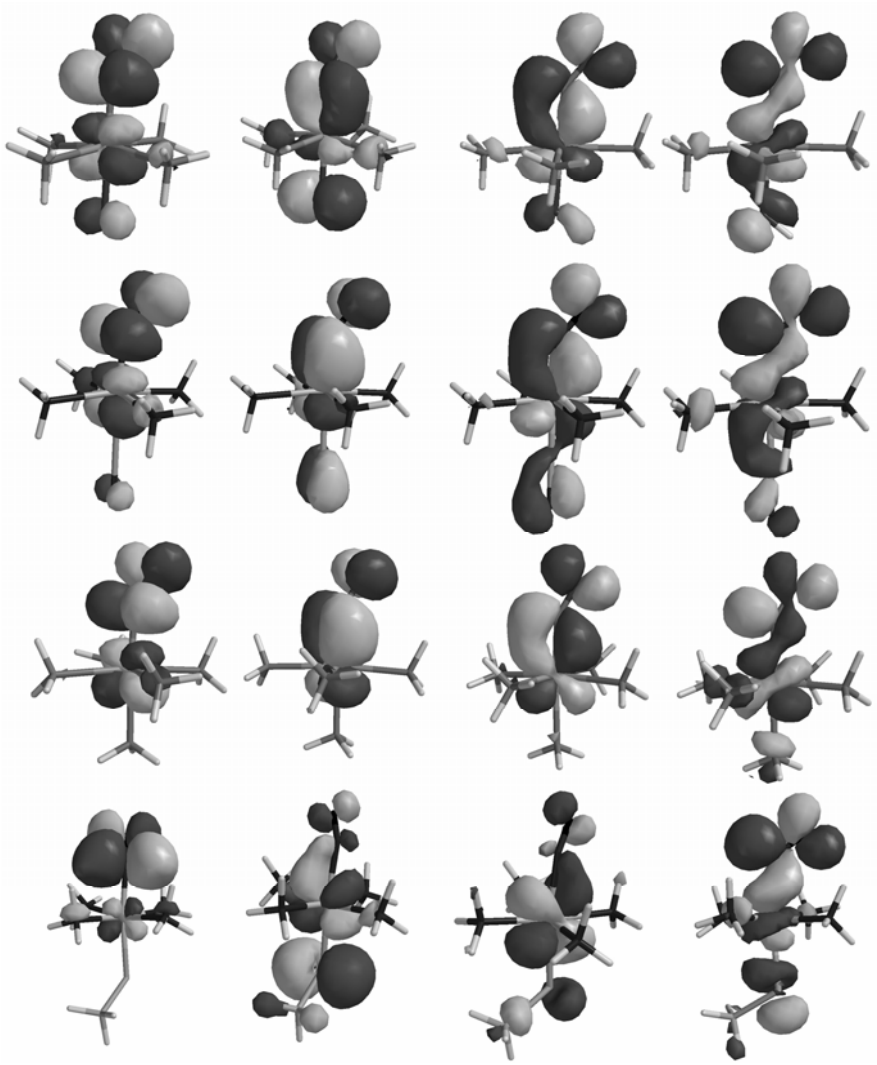

Fig. 3 – Frontier molecular orbitals for S=3/2 SOR $[FeNO]^7$ with various axial ligands (first row: hydroxide, second row: cyanide, third row: ammonia, fourth row: thiolate). Shown from left to right are π, π*, σ, and σ* molecular orbitals resulted from mixing of iron d_{xz} and d_{yz} with the two NO π* orbitals.[31]

S=3/2 $[FeNO]^7$ adducts were described as extremely covalent, which would render futile any attempt to describe them as either Fe(II)-NO or Fe(III)-NO^- limiting structures.[32] On the other hand, the current consensus is that all S=3/2 $[FeNO]^7$ complexes, including SOR-NO, are best described as S=5/2 Fe(III) antiferromagnetically coupled to S=1 NO^-.[26,27,33,34] None of these theories appears to apply for the SOR-NO case. Fig. 3 shows that, due to the thiolate-iron π interaction, the iron-NO interaction in SOR-NO is significantly less covalent than in other S=3/2 $[FeNO]^7$ complexes. Brief inspection of the frontier orbitals of thiolate-ligated SOR-NO (diagram shown as Supporting Information) reveals the iron d_{z2} and d_{x2-y2} to be formally empty, with d_{xy} and d_{yz} doubly-occupied and d_{xz} singly-occupied. Thus, SOR-NO is well described as S=1/2 Fe(III) + S=1 NO^-. This contradicts the previous proposal[8] that the iron in SOR-NO is best described as S=5/2 Fe(III), as well as the ensuing conclusion,[8] that the existence of a S=3/2 SOR-NO adduct is proof for a S=5/2 Fe(III)-OOH adduct in the SOR catalytic cycle. An extreme resilience of the thiolate-iron interaction is revealed by our study of the SOR-NO adduct. Comparing the magnitudes of the trends in Tables 1 and 3, NO appears to be a weaker ligand than peroxide, thereby allowing more sensitive probing of the thiolate trans effect. Thus, the present study yet again confirms the usefulness of probing enzyme active sites with substrate mimics; such mimics may expose and explore features of the active sites that cannot be readily deduced from analysis of true catalytic intermediates.

We will end the discussion by pointing out that the proton affinity of the ferric-peroxo models is some 200 kca/mol higher in the mode featuring a thiolate axial ligand, compared to the modes featuring a neutral amine ligand. This thermodynamic factor may well become the key reason why an enzyme like SOR would prefer an axial cysteinate ligand: such a ligand would distinctly accelerate peroxide protonation, thus allowing for a more efficient turnover.

CONCLUSIONS

Reporting DFT geometry optimization data on ferric-(hydro)peroxo models of the SOR active site, with the axial thiolate replaced by various neutral or anionic ligands, we find evidence for only a moderate thiolate trans effect on the peroxo (hydro)ligand. We then report DFT data on the nitric oxide adduct of the SOR site, where a dramatic trans effect of the thiolate is found. Examining SOR-NO models with different axial ligands, we assign the trans effect to a strong S-Fe π interaction. SOR-NO $[FeNO]^7$ is best described as S=1/2 Fe(III) + S=1 NO^-.

Acknowledgements: Prof. I. Silaghi-Dumitrescu is thanked for helpful discussions. Funding from the Roumanian Academy (63/28.08.2007) is gratefully acknowledged.

REFERENCES

1. F. J. Jenney, M. Verhagen, X. Cui and M. Adams, *Science*, **1999**, *286*, 306-308.
2. D. M. J. Kurtz and E. Coulter, *J. Biol. Inorg. Chem.*, **2002**, *6.*, 653-658..
3. M. Sono, M. P. Roach, E. D. Coulter and J. H. Dawson, *Chem. Rev.*, **1996**, *96*, 2841-2887.
4. E. Coulter, J. Emerson, D. J. Kurtz and D. Cabelli, *J. Am. Chem. Soc.*, **2000**, *122*, 11555-11556.
5. R. Silaghi-Dumitrescu and I. Silaghi-Dumitrescu, *Rev. Roum. Chim.*, **2004**, *49*, 257-268.
6. J. H. Dawson, R. H. Holm, R. H. Trudell, G. Barth, R. E. Linder, E. Nunnernberg, C. Djerassi and S. C. Tang, *J. Am. Chem. Soc.*, **1976**, *98*, 3707.
7. F. Ogliaro, S. deVisser and S. Shaik, *J. Inorg. Biochem.*, **2002**, *91*, 554-567.
8. M. D. Clay, C. A. Cosper, F. E. Jenney, M. W. Adams and M. K. Johnson, *Proc. Natl. Acad. Sci. USA*, **2003**, *100*, 3796-3801.
9. J. A. Kovacs, *Chem. Rev.*, **2004**, *104*, 825-48.
10. R. Silaghi-Dumitrescu, *Eur. J. Inorg. Chem.*, **2003**, 1048-1052.
11. R. Silaghi-Dumitrescu, I. Silaghi-Dumitrescu, E. D. Coulter and D. M. Kurtz, Jr., *Inorg. Chem.*, **2003**, *42*, 446-56.
12. D. L. Harris and G. H. Loew, *J. Am. Chem. Soc.*, **1998**, *120*, 8941-8948.
13. J. Shearer, R. C. Scarrow and J. A. Kovacs, *J. Am. Chem. Soc.*, **2002**, *124*, 11709-11717.
14. A. D. Becke, *Phys. Rev.*, **1988**, 3098-3100.
15. J. P. Perdew, *Phys. Rev.*, **1986**, *B33*, 8822-8824.
16. Spartan 5.0, Wavefunction, Inc., 18401 Von Karman Avenue Suite 370, Irvine, CA 92612 U.S.A.
17. R. Silaghi-Dumitrescu, *unpublished results*.
18. A. Yeh, Y. Hu, F. J. Jenney, M. Adams and D. Rees, *Biochemistry*, **2000**, *39*, 2499-2508.
19. A. Coelho, P. Matias, V. Fulop, A. Thompson, A. Gonzalez and M. Carrondo, *J. Biol. Inorg. Chem.*, **1997**, *2*, 680-689.
20. N. Lehnert, R. Y. N. Ho, L. J. Que and E. I. Solomon, *J. Am. Chem. Soc.*, **2001**, *122*, 12802-12816.
21. N. Lehnert, R. Y. N. Ho, L. J. Que and E. I. Solomon, *J. Am. Chem. Soc.*, **2001**, *123*, 8271-8290.
22. R. Silaghi-Dumitrescu and I. Silaghi-Dumitrescu, *Rev. Roum. Chim.*, **2004**, *49*, 257-268.
23. D. L. Harris, *Curr. Opin. Chem. Biol.*, **2001**, *5*, 724-735.
24. R. Silaghi-Dumitrescu and I. Silaghi-Dumitrescu, *J Inorg Biochem*, **2006**, *100*, 161-6.
25. J. H. Enemark and R. D. Feltham, *Coord. Chem. Rev.*, **1974**, *13*, 339.
26. C. A. Brown, M. A. Pavlovski, T. E. Westre, Y. Zhang, B. Hedman, K. O. Hodgson and E. I. Solomon, *J. Am. Chem. Soc.*, **1995**, *117*, 715-732.
27. C. Hauser, T. Glasser, E. Bill, T. Weyhermuller and K. Wieghardt, *J. Am. Chem. Soc.*, **2000**, *122*, 4352-4365.
28. T. W. Hayton, P. Legzdins and W. B. Sharp, *Chem. Rev.*, **2002**, *102,* 935-992.
29. R. Silaghi-Dumitrescu, *Rev. Chim.*, **2004**, *49*, 496-498.
30. Constraining the Fe-S distance to be longer by 0.2 A than this equilibrium value did not result in any shortening of the Fe-NO bond below 2.0 A. On the other hand, replacing the axial ligands with a porphyrin resulted in further elongation of the Fe-NO bond by 0.1 A; the latter result is of little experimental relevance, since such porphyrin adducts are always S=1/2 as opposed to S=3/2 examined here.
31. Mixing of iron d_{z2} with the Fe-NO π^* (far right in diagram) occurs to some extent in all models, but is most visible with the thiolate.
32. J. H. Rodriguez, Y. M. Xia and P. G. Debrunner, *J. Am. Chem.Soc.*, **1999**, *121*, 7846-7863.
33. T. A. Jackson, E. Yikilmaz, A. F. Miller and T. C. Brunold, *J. Am. Chem. Soc.*, **2003**, *125*, 10833-10845.
34. R. Silaghi-Dumitrescu and D. M. Kurtz , Jr., *Chemtracts Inorg. Chem.*, **2003**, *16*, 468-473.